IOCN 2022

MDPI

Proceeding Paper

Synthesis and Study of Beeswax-Carbon Nanotubes-Recycled Paperboard Nanocomposite †

Tejashree Amberkar * and Prakash Mahanwar

Department of Polymer and Surface Engineering, Institute of Chemical Technology, Mumbai 400019, India; pa.mahanawar@ictmumbai.edu.in

* Correspondence: tejuamberkar@yahoo.co.in.

† Presented at the 3rd International Online Conference on Nanomaterials, 25 April–10 May 2022 Available online: https://iocn2022.sciforum.net/

Abstract: Beeswax is a bio-based organic phase change material. It undergoes solid to liquid phase transition at 61 °C with the phase transition enthalpy of 216 J/g. The high thermal energy storage enthalpy of beeswax is suitable for maintaining constant temperature. However, the low thermal conductivity of beeswax limits the heat transfer rate. Also, beeswax should be form-stabilized to minimize leakage in the molten state. In this study, the thermal conductivity of beeswax was improved with carbon nanotube (CNT) incorporation. The leakage of molten beeswax was minimized by coating it on recycled paperboard. The beeswax-CNT-recycled paperboard nanocomposite was further coated with silicone adhesive. It ensured the retention of molten wax. FTIR spectrum and SEM morphology of nanocomposite confirm physical dispersion of CNT into the matrix. DSC analysis of nanocomposites showed reduction of TES enthalpy to 98.52 J/g.

Keywords: phase change material; thermal energy storage; carbon nanotubes: beeswax; latent heat

Citation: Amberkar, T.; Mahanwar, P. Synthesis and Study of Beeswax-Carbon Nanotubes-Recycled Paperboard Nanocomposite. *Biol. Life Sci. Forum* **2022**, 2, x. https://doi.org/10.3390/xxxxx

1. Introduction

Organic phase change materials (PCMs) have low thermal conductivity [1]. The low thermal conductivity of PCM lower speed of heat conduction. Many researchers have used different strategies for improving heat conductivity of PCM. The low thermal conductivity of PCM have been improved with various carbon-based and metal-based nanomaterials [2]. Inclusion of nanomaterials improve thermal conductivity of synthesized nanocomposite. But it also changes density, chemical and mechanical properties of composite. The carbon-based nanomaterials have density near to 2.26 $g.cm^{-3}$ which is close to density of organic PCMs [3]. On the other hand, metal-based nanomaterials have high density. Dispersing dense metal nanoparticles uniformly in matrix is challenging task. Non-uniform dispersion gives anisotropic thermal properties. The carbon-based nanomaterials are more stable to chemical and thermal treatments. Such processes are often involved in form stabilization of PCM. Thus, carbon-based nanomaterials are preferred over metal-based nanomaterials for improving thermal conductivity of organic PCMs.

The carbon-based nanomaterials come in different morphologies [4]. The morphology affects aspect ratio, percolation and heat transfer rout in composite. Tao, Lin and He studied thermal properties of carbon-based nanocomposites with four morphologies [5]. Fullerene C_{60} possesses spherical morphology. The spherical fullerene structure lowered thermal conductivity in nanocomposite. The geometry of graphene nanoplatelets can be described as 2D-square sheet. Graphene nanocomposites had comparatively lower heat storage enthalpy. The single walled carbon nanotubes (SWCNT) and the multiwalled carbon nanotubes (MWCNT) have short cylindrical and long cylindrical morphology respectively. Out of all nanocomposites, CNT nanocomposites showed highest increase in ther-

mal conductivity. This structure helps in hindering leakage of molten beeswax. The thermal conductivity values were slightly higher for SWCNT composites. Considering cost factor of preparing SWCNT and MWCNT, MWCNT nanocomposites are suitable for practical applications. The nanocomposites require additional container to achieve customized shape for application. Polymeric materials serve as good matrix for PCM-CNT nanocomposite. Ma et al. [6] used bottlebrush crystalline silicon polymers for incorporating paraffin wax and CNTs. This polymeric matrix added material specific properties suitable for application. The 3D polymer network is flexible and superhydrophobic. Presence of CNT improved thermal conductivity of composite. Such multifunctional composite finds application in wearable devices, electronic machines, building materials, etc.

Beeswax (BW) is an eco-friendly PCM. The low carbon footprint associated with BW production makes it a promising candidate for thermal energy storage (TES) applications. Its phase transition temperature is suitable for food packaging applications [7,8]. The use of thermal energy storing beeswax-recycled paperboard sheets inside insulated packaging container help in maintaining desired temperature for longer time. But beeswax is an organic PCM with low thermal conductivity 0.25–0.3 $W \cdot m^{-1} \cdot K^{-1}$ [9,10]. In this study, BW-MWCNT nanocomposite is prepared for is prepared for improving thermal performance of packaging container. The high thermal conductivity and low density of MWCNTs are suitable for dispersing CNTs in BW matrix. BW-CNT nanocomposite will possess high thermal conductivity helping in improving heat transfer rate. BW-CNT nanocomposite can be coated on recycled paper sheet of required shape in packaging application. The thermal performance of BW-CNT-recycled paperboard composite sheet was studied in insulated packaging container.

2. Materials and Methods

2.1. Materials

Beeswax was procured from anaha™, Goa, India. MWCNTs with diameter 30–50 nm and length 10–30 μm were purchased from Sisco research laboratories Pvt. Ltd., Mumbai, India. Commercially available uncoated paper sheets were obtained from the local market in Mumbai, India. Tween 80 was obtained from SD fine chemicals private limited, Mumbai, India. Room temperature vulcanizing silicone adhesive was purchased from Astral adhesives, Gujrat, India. Sodium benzoate was purchased from Shree Lakshmi chemicals, Banglore, India. For the experiments, DI water was used. Arduino UNO, Adiy™, Mumbai, India, was used to build and programme temperature data logger. Expanded polystyrene insulation sheet, two bigger cartons (1 × 13 × 25 cm^3) and two smaller cartons (16 × 10 × 22.5 cm^3) were purchased from a local market in Mumbai, India.

2.2. Method of Preparation

The suspension of CNT in DI water was prepared with two drops of emulsifier by ultrasonication for 1 h. The BW-CNT composites were made by adding suspension into mixture of molten beeswax, one weight percent emulsifier, and two weight percent antimicrobial agent. The nanocomposites with CNT concentrations 0.02 wt.%, 0.04 wt.%, 0.06 wt.% and 0.08 wt.% were prepared. The prepared solution was heated at 70 °C for 30 min under magnetic stirring in closed container. The water was evaporated from the solution at 100 °C. The mixture was again homogenized at 70 °C for 30 min under ultrasonication. The molten mixture was coated on paper sheet. The papers were dried at room temperature (RT). The silicon adhesive coat was applied after 24 h. The prepared sheets were further dried for seven days.

2.3. Characterization Techniques

2.3.1. T-History

The setup consisted of two identical test tubes with water as reference material and sample PCM nanocomposite. The test tubes were heated to 70°C and their cooling process

at RT was recorded with temperature sensors. The temperature-time graph of the reference and BW-CNT composites were plotted with obtained data.

The specific heat, heat of fusion and thermal conductivity of the solid PCM are determined using the following formula [11]

$$c_p = \frac{m_R * c_{p,R} + m_t * c_{p,t}}{m_p} \times \frac{A_p}{A_R} - \frac{m_t * c_{p,t}}{m_p}$$

where m_R is mass of reference material, m_t is mass of tube material, m_p is mass of PCM, c_p is specific heat capacity of PCM sample, $c_{p,R}$ is specific heat capacity of reference material, $c_{p,t}$ is specific heat capacity of tube material, A_p is the area under the cooling curve of PCM and A_R is the area under the cooling curve reference material.

Heat of the fusion can be calculated using the formula [12]

$$H_m = \frac{m_R * c_{p,R} + m_t * c_{p,t}}{m_p} \times \frac{A_p}{A_R}(T_0 - T_{m,1}) - \frac{m_t * c_{p,t}}{m_p}(T_0 - T_{m,2})$$

where m_R is mass of reference material, m_t is mass of tube material, m_p is mass of PCM, c_p is specific heat capacity of PCM sample, $c_{p,R}$ is specific heat capacity of reference material, $c_{p,t}$ is specific heat capacity of tube material, T_0 is the temperature at the start of experiment, $T_{m,1}$ is the temperature at the start of phase transition process of PCM, $T_{m,2}$ is the temperature at the end of phase transition process of PCM, A_p is the area under the cooling curve of PCM and A_R is the area under the cooling curve reference material.

Thermal conductivity of the solid PCM was calculated using the formula [11]

$$k_p = [1 + \frac{c_p(T_m - T_\infty)}{H_m}]/4\,[\frac{t_f(T_m - T_\infty)}{R^2 \rho_p H_m}]$$

where k_p is the effective thermal conductivity of the PCM, c_p is the specific heat of the PCM, ρ_p is the density of the PCM, R is the radius of test tube, H_m is the heat of fusion of PCM as obtained from the DSC results and T_m & T_∞ is the temperature of melting and atmosphere respectively. Time of solidification of the molten PCM is denoted by t_f.

2.3.2. Scanning Electron Microscopy

The scanning electron microscope (SEM) was used to examine the morphology of the nanocomposites. The morphology was studied using FEI Quanta 200 SEM model.

2.3.3. Fourier Transform Infrared Spectroscopy

The samples were scanned in the Fourier Transform Infrared (FTIR) spectroscope in 4000–500 cm^{-1} range using a Bruker Alpha spectrometer in attenuated total reflectance spectra mode.

2.3.4. Differential Scanning Calorimetry

The differential scanning calorimeter (DSC) DSC 3, Mettler Toledo, Tokyo was used to analyze thermal properties of composite in temperature range 25 °C to 100 °C. The heating rate of 10 °C/min was achieved in nitrogen atmosphere.

2.3.5. Heat Release Performance in Carton

The heat release performance of prepared nanocomposite sheets was checked with an assembly depicted in published paper [8]. The thermal performance of empty control sample and filled PCM sheet sample was studied. The glasses of boiled water were placed in smaller cartons and consequently in larger cartons as shown in Figure 1. The empty space between the smaller and larger carton walls was filled with polystyrene insulation sheets and 60 gm PCM nanocomposites sheets. The drop in temperature of water was measured with data logger.

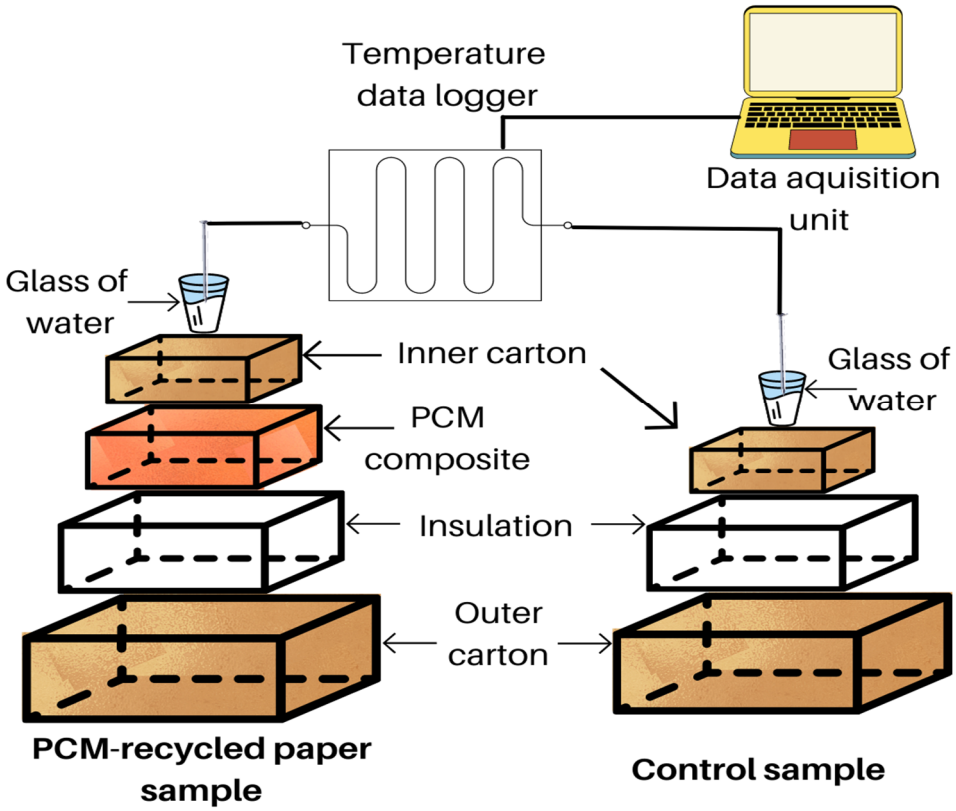

Figure 1. Assembly for heat release performance testing [8].

3. Results and Discussion

The T-history method performed on BW and BW-CNT composites gave temperature-time profiles which are shown in Figure 2. The presence of CNTs modified temperature-time profiles. The values H_m, thermal conductivity and time of phase transition calculated from these profiles are shown in Table 1. The thermally conductive CNTs form conductive path networks for faster heat transfer in BW composite structures. With 0.02% addition in CNT concentration, phase transition time decreased by 5.08% 11.53% 13.78% and 15.93% respectively. This reduction was smaller for BW-0.06 CNT and BW-0.08 CNT composites. The thermal conductivity of BW-CNT composites increases with increase in CNT concentration. The values can be observed in Table 1. This increase was less for 0.06% and 0.08% CNT concentration. The possible reason of these anomalous values can be agglomeration of CNTs. The enthalpy of crystalline structure of beeswax reduced slightly with the presence of CNTs. Increase in CNT concentration decreases H_m value by small amount. This change is within 3% of pure beeswax enthalpy.

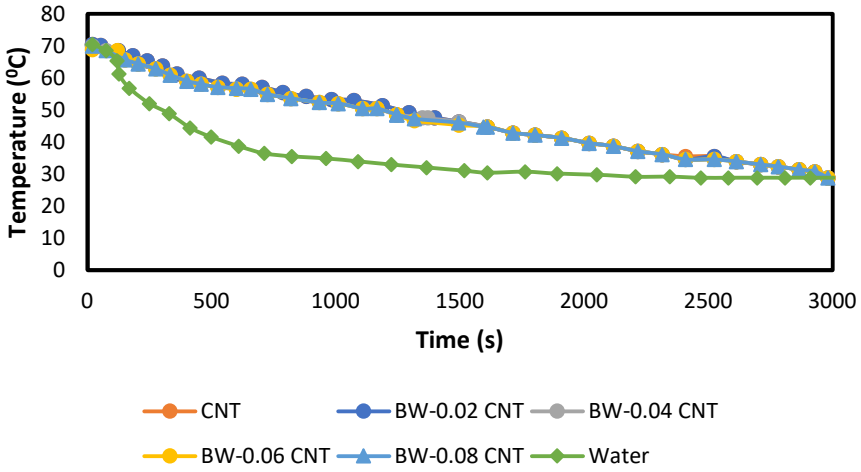

Figure 2. Temperature-time profiles of BW and BW-CNT composites.

Table 1. T-history test results.

Composition	Time of Phase Transition (s)	Decrease in Time of Phase Transition (%)	Thermal Conductivity ($W \cdot m^{-1} \cdot K^{-1}$)	Increase in Thermal Conductivity (%)	H_m (J/g)
BW	1023	0	0.284	0	220.71
BW-0.02 CNT	971	5.08	0.298	4.92	220
BW-0.04 CNT	905	11.53	0.308	8.45	217.72
BW-0.06 CNT	882	13.78	0.312	9.86	215.92
BW-0.08 CNT	860	15.93	0.315	10.91	214.55

SEM analysis of the BW-0.04 CNT and BW-0.06 CNT composites is represented in Figure 3. Smooth morphology is observed in Figure 3a. The spots in Figure 3b might be due to CNTs agglomeration. The surfactant concentration was not sufficient to disperse CNTs in BW-0.06 composite. The agglomeration of CNTs creates non-uniform heat transfer network in composite. Thus, thermal properties of BW-0.06 CNT and BW-0.08 CNT did not improve significantly. The BW-0.04 CNT composite has good heat storage enthalpy and high thermal conductivity. It was selected for improving thermal performance of packaging container.

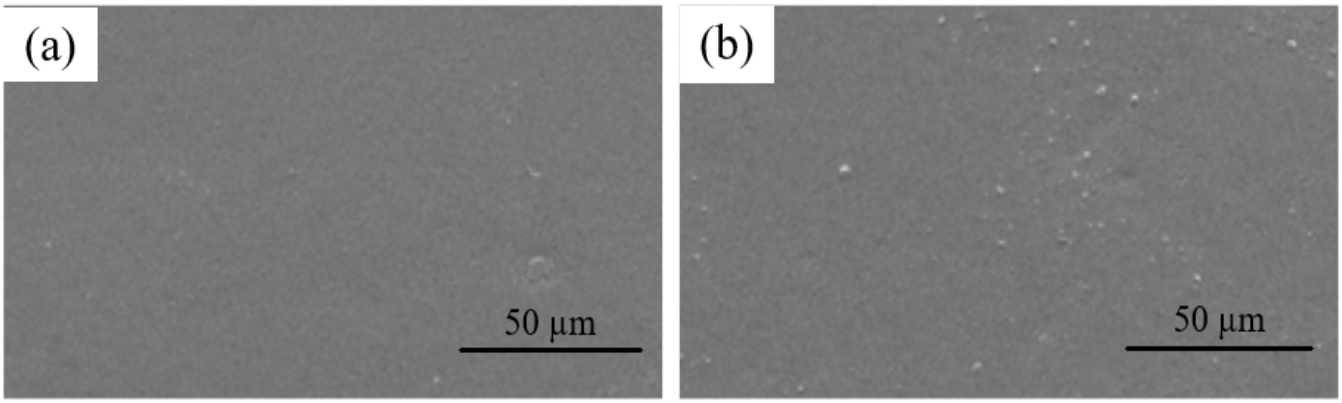

Figure 3. Morphology of (**a**) BW-0.04 CNT and (**b**) BW-0.06 CNT.

Beeswax's FTIR spectrum shown by Figure 4a reveals the chemical structures of its constituents. The peak at 718 cm^{-1} corresponds to rocking vibrations of long-chain hydrocarbons (HCs). The C-O stretching arising from the aromatic ester represented by the band at 1365 cm^{-1}. The C-H bending of aliphatic HCs is responsible for the peak at 1463 cm^{-1}. The band at 1691 cm^{-1} represented stretching vibrations emanating from the C=O bond in aromatic acid. The peaks at 2846 cm^{-1} and 2920 cm^{-1} arise from stretching vibrations of the CH_2 group. The BW-0.04 CNT spectrum in Figure 4b contained all the typical peaks of beeswax. No new peaks were observed. This confirms physical dispersion of CNTs into the beeswax matrix.

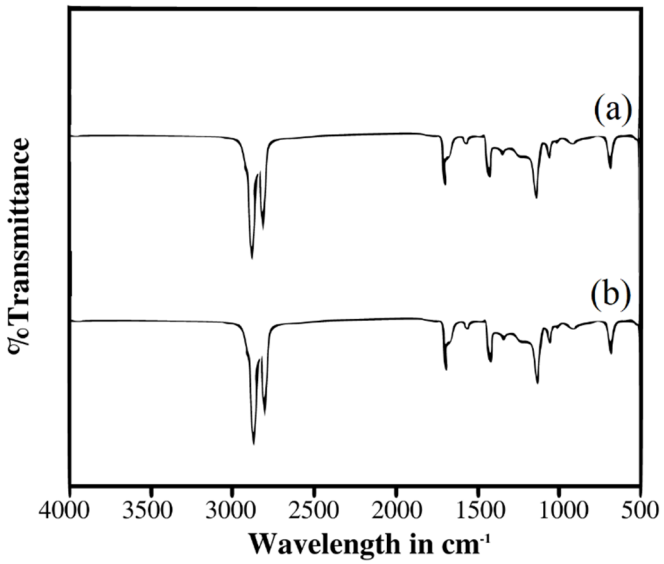

Figure 4. FTIR spectra of (**a**) BW and (**b**) BW-0.04 CNT**.**

The heat release test was used to investigate the effectivity of PCM nanocomposite sheets on the temperature of confined water. The temperature-time curve of water in the PCM nanocomposite sheet sample and the control sample carton is shown in Figure 5. Temperature measurements were taken at the same time for both samples. Temperature measurements for the samples began at 88 °C. Initially for 1872 s, PCM nanocomposite sample and control sample reduced temperature of water to around 62 ^{0}C with similar temperature-time profile. At 4031 s, water in control assembly reached ambient temperature. It took less time for the control assembly to attain ambient temperature. The heat storage enthalpy of BW and BW-0.04 CNT composite was 216.09 J/g and 98.52 J/g, respectively, in DSC. The TES phenomenon of PCM is confirmed by the increase in time to attain ambient temperature for PCM nanocomposite sheets. The interior temperature remained higher for longer in the composite assembly than in the control assembly. The heat transfer from the PCM to the interior chamber is responsible for the increased temperature inside the carton. In the event of a delayed supply, this phenomenon can be employed to maintain a greater temperature.

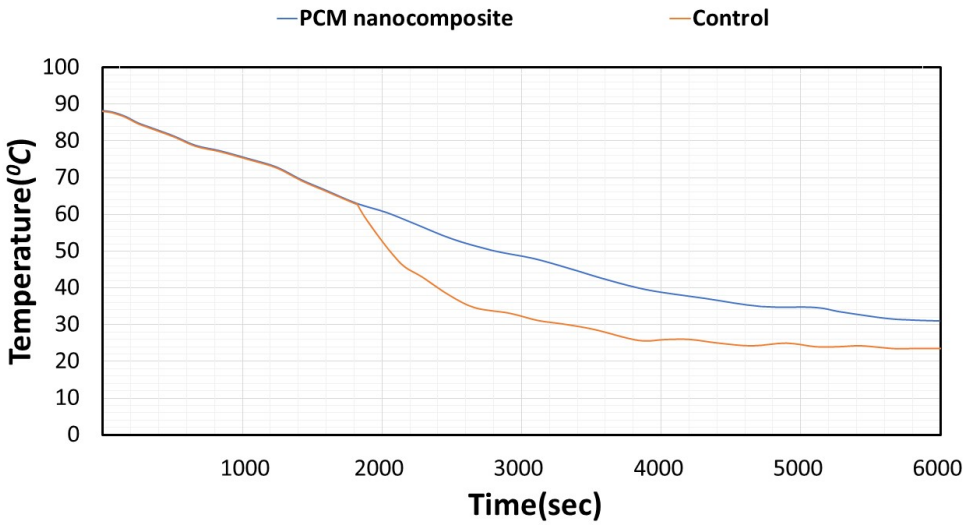

Figure 5. Temperature-time profile of control sample and PCM nanocomposite sample.

4. Conclusions

T-history analysis showed thermal conductivity and heat storage enthalpy of BW-0.04 CNT composite as 0.308 $W \cdot m^{-1} \cdot K^{-1}$ as and 217.72 J/g respectively. The CNT concentration of 0.04% showed good dispersion in beeswax in SEM analysis. Physical mixing of PCM and CNT was confirmed by FTIR. DSC examination of the BW-0.04 CNT paper composite revealed good heat storage capabilities with melting enthalpy of 98.52 J/g. The use of PCM nanocomposite sheets can lengthen the time it takes to maintain food temperature close to the composite's phase transition temperature.

Author Contributions: Writing—original draft preparation, T.A.; writing—review and editing, P.M. All authors have read and agreed to the published version of the manuscript.

Funding: This work is funded by AICTE National Doctoral Fellowship Scheme sanctioned vide letter F No: 12-2/2019-U1 provided by the Ministry of Human Resource Development, Government of India.

Institutional Review Board Statement: Not applicable.

Informed Consent Statement: Not applicable.

Data Availability Statement: The data presented in this study are available on request from the corresponding author.

Acknowledgments: The authors acknowledge research facilities provided by Institute of Chemical Technology, Mumbai.

Conflicts of Interest: The authors declare no conflict of interest.

References

1. Pielichowska, K.; Pielichowski, K. Phase change materials for thermal energy storage. *Prog. Mater. Sci.* **2014**, *65*, 67–123. https://doi.org/10.1016/j.pmatsci.2014.03.005.
2. Lin, Y.; Jia, Y.; Alva, G.; Fang, G. Review on thermal conductivity enhancement, thermal properties and applications of phase change materials in thermal energy storage. *Renew. Sustain. Energy Rev.* **2018**, *82*, 2730–2742. https://doi.org/10.1016/j.rser.2017.10.002.
3. Zhang, Q.; Luo, Z.; Guo, Q.; Wu, G. Preparation and thermal properties of short carbon fibers/erythritol phase change materials. *Energy Convers. Manag.* **2017**, *136*, 220–228. https://doi.org/10.1016/j.enconman.2017.01.023.
4. Huang, X.; Alva, G.; Jia, Y.; Fang, G. Morphological characterization and applications of phase change materials in thermal energy storage: A review. *Renew. Sustain. Energy Rev.* **2017**, *72*, 128–145. https://doi.org/10.1016/j.rser.2017.01.048.
5. Tao, Y.B.; Lin, C.H.; He, Y.L. Preparation and thermal properties characterization of carbonate salt/carbon nanomaterial composite phase change material. *Energy Convers. Manag.* **2015**, *97*, 103–110. https://doi.org/10.1016/j.enconman.2015.03.051.

6. Ma, J.; Ma, T.; Duan, W.; Wang, W.; Cheng, J.; Zhang, J. Superhydrophobic, multi-responsive and flexible bottlebrush-network-based form-stable phase change materials for thermal energy storage and sprayable coatings. *J. Mater. Chem. A* **2020**, *8*, 22315–22326. https://doi.org/10.1039/d0ta07619h.
7. Amberkar, T.; Mahanwar, P. Composite Phase Change Material for Improving Thermal Protection Performance of Insulated Packaging Container. *Int. J. Eng. Trends Technol.* **2022**, *70*, 59–64. https://doi.org/10.14445/22315381/IJETT-V70I2P209.
8. Amberkar, T.; Mahanwar, P. Study and Characterization of Phase Change Material-Recycled Paperboard Composite for Thermoregulated Packaging Applications. *Mater. Proc.* **2021**, *7*, 17. https://doi.org/10.3390/iocps2021-11208.
9. Amin, M.; Putra, N.; Kosasih, E.A.; Prawiro, E.; Luanto, R.A.; Mahlia, T.M.I. Thermal properties of beeswax/graphene phase change material as energy storage for building applications. *Appl. Therm. Eng.* **2017**, *112*, 273–280. https://doi.org/10.1016/j.applthermaleng.2016.10.085.
10. Mishra, D.K.; Bhowmik, S.; Pandey, K.M.; Hui, W. Analysis of Heat Transfer Rate for Different Annulus Shape Properties-Enhanced Beeswax-Based Phase Change Material for Thermal Energy Storage. *Math. Probl. Eng.* **2022**, *2022*, 3472. https://doi.org/10.1155/2022/6123472.
11. Venkitaraj, K.P.; Suresh, S.; Praveen, B.; Arjun, V.; Sreeju, C. Pentaerythritol with alumina nano additives for thermal energy storage applications. *J. Energy Storage* **2017**, *13*, 359–377. https://doi.org/10.1016/j.est.2017.08.002.
12. Yinping, Z.; Yi, J.; Yi, J. A simple method, the-history method, of determining the heat of fusion, specific heat and thermal conductivity of phase-change materials. *Meas. Sci. Technol.* **1999**, *10*, 201–205. https://doi.org/10.1088/0957-0233/10/3/015.